LRE Chamber Wall Optimization
Using Plane Strain and Generalized Plane Strain Models

Jörg R. Riccius*, Evgeny B. Zametaev† and Oskar J. Haidn‡
German Aerospace Center (DLR), Lampoldshausen, 74239, Germany

and

Christian Gogu §
Ecole Nationale Supérieure des Mines de Saint Etienne, 42023, France

A method for the optimization of rocket combustion chamber (combustion chamber) walls with respect to the life time is presented. This method can be split into four main parts: P1) Determination of the thermal field within the combustion chamber wall and the cooling channel during the hot run phase by a steady state thermo-fluid mechanical analysis; P2) Analysis of the nonlinear deformation of the combustion chamber wall under cyclic thermal and mechanical loading using a 2d plane strain or a 2d generalized plane strain model; P3) Estimation of the life time of the combustion chamber wall by a post processing method and P4) Application of a mathematical optimization procedure (gradient free or Conjugate Gradient method). This strategy is used to analyse the thermal load induced deformation process and life time of a typical rocket combustion chamber and to optimise selected geometry parameters of the combustion chamber wall.

I. Introduction

The combustion chamber liner of a cryogenic rocket engine is exposed to serious thermal loads due to the large temperature differences between the stiff close-out which is typically at liquid hydrogen temperature and the hot gas side wall which may reach 900 K. The induced thermal stresses generally are beyond the elastic limit of the copper alloy and the amount of plastic deformation may reach up to 2%. Fig. 1 shows a cut through the liner with the typical failure mechanism, the dog-house effect. In addition to these thermal loads, the liner material is subject to other chemical and physical attacks which weaken the material strength. The available tools for component life prediction have to be continuously updated and validated in order to meet the requirements for the design of a reusable space transportation system.

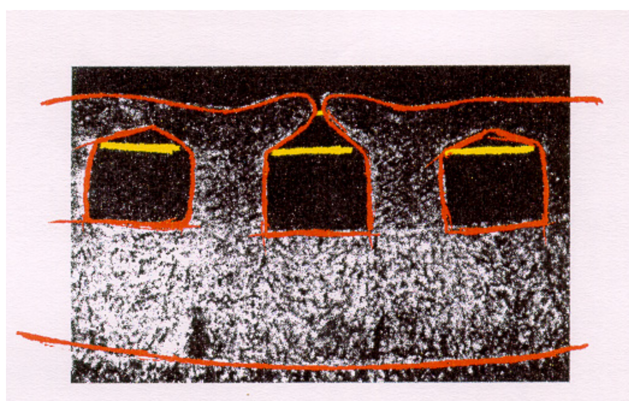

Figure 1. Typical cooling channel failure mode.

A. Motivation

The requirements regarding reliability and performance of cryogenic liquid rocket engines in combination with the need to continuously reduce both production and operational cost has led to the idea of reusable space

* Head of Fluids & Structures Group, Institute of Space Propulsion, Member AIAA.
† Senior Finite Element analyst, Institute of Space Propulsion.
‡ Head of Technology, Institute of Space Propulsion, Associate Fellow AIAA.
§ Graduate student, Department of materials and structures, AIAA student member.

transportation systems. With 50 or more cycles being a typical life requirement for such a system and nowadays combustion chambers having cycles-to-failure numbers of about 20 or less, the current research and technology activities at DLR aim at a detailed understanding of the failure mechanisms and the development of a verified tool for combustion chamber life prediction.[1]

An earlier investigation aiming into the optimization of the cooling channel geometry has shown that the applied material model (isotropic or kinematic hardening) and life time estimation method have a dramatic influence on the optimization result.[2] This work also demonstrated the importance of the proper choice of elasto-plastic material parameters and the accurate description of the material in an appropriate non-linear material model. With these findings in mind, a series of material tests was performed.[3,4] In the current contribution, the influence of the 2 d model (plane strain or generalized plane strain) on the optimization is considered.

II. General Approach

An optimization of given combustion chamber wall parameters is obtained by a successive (one way coupled) analysis of the following sub problems:

- 1d stationary thermo-fluid-mechanical analysis of the system hot gas / combustion chamber wall / coolant
- 2d thermal analysis of the combustion chamber wall during the hot run
- 2d nonlinear structural analysis of the combustion chamber wall under cyclic thermal and mechanical loading
- post processing life time estimation of the combustion chamber wall
- usage of the estimated number of cycles until failure as an objective function for a mathematical optimization procedure

On the hot gas side, the Bartz equation[5] is applied and film coefficients from experiments are chosen. On the coolant side, a one-dimensional thermo-fluid mechanical approach is used, taking into account empirical models for the heat transfer and fluid mechanical losses. The circumferential variation of the local wall heat flux into the cooling channel is taken into account by using a two dimensional FEM model for the simulation of the thermal field within the wall structure. No stratification effects of the cooling channel flow are taken into account in the currently presented work. However, thermal stratification models have been successfully implemented at DLR Lampoldshausen and applied for pure thermo-fluid-mechanical analyses.[6] In the framework of a comparative study, the film coefficients, obtained by the one dimensional thermo-fluid-mechanical analysis, are used to perform either a 2d thermal FEM analysis of the combustion chamber wall.

The resulting thermal fields are used as boundary conditions for a 2d plane strain or a 2d generalized plane strain analysis of the combustion chamber wall. A standard multilinear elasto-plastic structural analysis method with the von Mises yield function and isotropic hardening is used to analyze the structural behavior of the combustion chamber wall under cyclic thermal and mechanical loading. For an analysis of the low cycle fatigue life of the combustion chamber wall, a simple post processing method is applied, taking into account cyclic and quasi static fatigue as well as the aging of the material. Two different optimization procedures are compared: a conjugate gradient method and a gradient free method.

III. THERMAL ANALYSIS

In this section, the applied boundary conditions and results of the thermal analysis of the combustion chamber wall are shown. The basic equations and the specification of the material parameters are described in detail in.[7]

A. Material parameters

The thermal conductivity λ and the heat capacity c are defined temperature dependent. A visualization of these parameter values and a description of the determination of them are given in Ref. 8.

B. Geometric assignment of boundary conditions

The geometric assignment of the thermal boundary conditions for the analyzed part of the chamber wall is given in Fig. 2 and the boundary conditions are described in Ref. 7.

IV. Nonlinear structural analysis

A. Basic equations for all considered material models

Only quasi stationary structural analyses were performed. Therefore, the momentum equation (1) is formulated without dynamic effects:

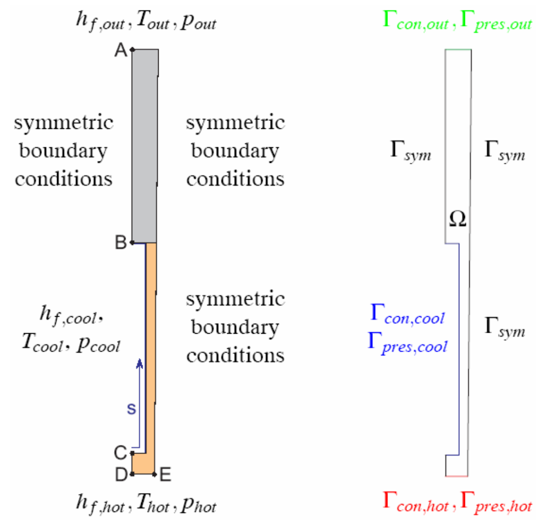

Figure 2. Geometric assignment of the thermal and mechanical boundary conditions.

$$\nabla \cdot \sigma = 0 , \qquad \forall x \in \Omega \tag{1}$$

with: σ … Cauchy stress tensor
x … spatial coordinate
Ω … analyzed domain as specified in Fig. 2

The stress tensor is given by the elastic strain relation (2)

$$\sigma = C : \varepsilon_{el} = C : (\varepsilon - \varepsilon_{pl} - \varepsilon_{th}) \tag{2}$$

$$\varepsilon_{th} = \alpha (T - T_{ref}) I_2 \tag{3}$$

with: ε … Green strain tensor
ε_{el} , ε_{pl} , ε_{th} … elastic, plastic and thermal strains
C … constitutive tensor as specified in the following subsection
E… modulus of elasticity
ν… Poisson´s ratio
α… thermal expansion coefficient
T… actual temperature of the combustion chamber wall
T_{ref} … reference (manufacturing) temperature of the combustion chamber wall

Whether plastic strains ε_{pl} develop or not is decided by the von Mises yield function f . For $f \le 0$, the problem behaves elastic and the plastic strains ε_{pl} stay constant. An increase of f to values larger than zero is prevented by building up plastic strains ε_{pl} which are determined by equation (4)

$$d\varepsilon_{pl} = \lambda \frac{\partial f}{\partial \sigma} \tag{4}$$

with: λ … plastic multiplier

Assuming isotropic hardening, the yield function $f(\sigma)$ does not only depend on the stress σ alone, but also on the performed plastic work:

$$f(\sigma,\kappa)=\|s\|-\sqrt{\frac{2}{3}}\sigma_{yield}(\kappa) \tag{5}$$

$$d\kappa=\sigma:d\varepsilon_{pl} \tag{6}$$

$$s=\sigma-\frac{tr(\sigma)}{3}I \tag{7}$$

$$\|s\|=\sqrt{s:s} \tag{8}$$

with: κ … performed plastic work
s … deviatoric stress tensor
$\sigma_{yield}(\kappa)$ … yield stress as a function of the performed plastic work

The yield stress $\sigma_{yield}(\kappa)$ is defined by the isotropic stress-strain curve for selected temperatures.

B. Differences of the 2d plane strain and generalized plane strain analyses

In order to obtain a comprehensive notation for the equation $\sigma=C:\varepsilon_{el}$, the components of the stress and the strain tensors are written as vectors and the constitutive tensor is written as a matrix in the following subsections.

1. 2d plane strain analysis

For the following equations it is assumed, that the working plane of the 2d models is the $x-y$ - plane. The basic assumption of the conventional plane strain model is a zero normal strain in thickness direction z of this model:

$$\varepsilon_{zz}=0 \qquad \forall x\in\Omega \tag{9}$$

As a result of the constant straining in thickness direction, the attached shear strain components also become zero:

$$\varepsilon_{zx}=0\,,\quad \varepsilon_{yz}=0 \qquad \forall x\in\Omega \tag{10}$$

These strain values result in the following stress values:

$$\sigma_{zx}=0\,,\qquad \sigma_{yz}=0\,,\qquad \sigma_{zz}=\frac{\lambda}{2(\mu+\lambda)}(\sigma_{xx}+\sigma_{yy}) \tag{11}$$

The remaining 2d plane strain matrix notation of the equation $\sigma=C:\varepsilon_{el}$ is then:

$$\begin{bmatrix}\sigma_{xx}\\ \sigma_{yy}\\ \sigma_{xy}\end{bmatrix}=\begin{bmatrix}2\mu+\lambda & \lambda & 0\\ & 2\mu+\lambda & 0\\ sym. & & \mu\end{bmatrix}\begin{bmatrix}\varepsilon_{xx}\\ \varepsilon_{yy}\\ 2\varepsilon_{xy}\end{bmatrix} \tag{12}$$

2. 2d generalized plane strain analysis with fixed rotations

A generalization of the basic assumption of the conventional plane strain model $\varepsilon_{zz}=0$ is a constant normal strain in thickness direction z of this model:

$$\varepsilon_{zz}=\varepsilon_{zz,const} \qquad \forall x\in\Omega \tag{13}$$

This leads to the same conclusion for the shear strain and shear stress components as in the conventional plane strain model:

$$\varepsilon_{zx}=0\,,\quad \varepsilon_{yz}=0\,,\quad \sigma_{zx}=0\,,\quad \sigma_{yz}=0 \qquad \forall x\in\Omega \tag{14}$$

However, one more equation is remaining in the matrix notation of the constitutive tensor of the 2d generalized plane strain model:

$$\begin{bmatrix} \sigma_{xx} \\ \sigma_{yy} \\ \sigma_{zz} \\ \sigma_{xy} \end{bmatrix} = \begin{bmatrix} 2\mu+\lambda & \lambda & \lambda & 0 \\ & 2\mu+\lambda & \lambda & 0 \\ & & 2\mu+\lambda & 0 \\ sym. & & & \mu \end{bmatrix} \begin{bmatrix} \varepsilon_{xx} \\ \varepsilon_{yy} \\ \varepsilon_{zz,const.} \\ 2\varepsilon_{xy} \end{bmatrix} \tag{15}$$

Although the values of ε_{xx}, ε_{yy} and ε_{xy} in general vary inside the analyzed domain Ω, the value of $\varepsilon_{zz,const}$ is constant over the entire 2d domain Ω. Therefore – independently on the total number of elements in the Finite Element model – only one additional global degree of freedom (the thickness change d_z of the model) is necessary for the 2d generalized plane strain analysis with fixed rotations in comparison with a conventional 2d plane strain analysis.

C. Pressure boundary conditions

As pressure boundary conditions, the values as given in Table 1 are taken.

D. Material parameters

The determination of the structural material parameters is described e.g. in Ref. 4.

E. Geometric assignment of boundary conditions

The geometric assignment of the boundary conditions is given in Fig. 2.

Table 1. Assumed pressure values for different steps of the loading cycle.

Stage	Time *[s]*	coolant pressure *[MPa]*	hot gas pressure *[MPa]*
pre cooling	0-2	2	0
hot run	2-4	13.4	10.0
post cooling	4-6	2	0
relaxation	6-8	0	0

V. Life time estimation

A post processing approach is chosen for the estimation of the life time of the combustion chamber wall. Three different failure mechanisms are taken into account: cyclic fatigue, quasi static (or ratcheting) fatigue and thermal aging.

A. Cyclic fatigue

The life time calculation for the cyclic fatigue part is based on experimental results[9] for the low cycle fatigue behavior of the combustion chamber wall material as shown in Fig. 3.

As a result of the calculations from the previous section, a cyclic total strain difference can be obtained for any considered position in the structure. From this strain difference and the fitted line from Fig. 3, the number of cycles until failure N_c can be obtained easily. The cyclic fatigue usage factor u_c is calculated as:

$$u_c = \frac{1}{N_c} \tag{1}$$

Usage factors are assumed to add up for each passed cycle and therefore, after N_c identical cycles, a usage factor of $N_c = 1.0$ is obtained, which indicates failure.

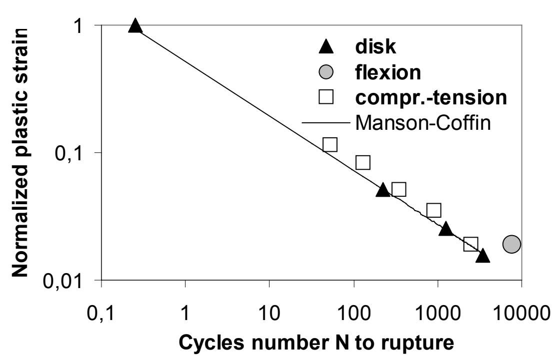

Figure 3. Normalized results of low cycle fatigue experiments for the analyzed combustion chamber wall material.

B. Quasi static fatigue

The quasi static (or ratcheting) usage factor u_{qs} is defined as:

$$u_{qs} = \frac{\max(0,(\varepsilon_{end} - \varepsilon_{begin}))}{\varepsilon_u} \tag{2}$$

with:

ε_{end} remaining strain after the considered cycle

ε_{begin} strain at the beginning of the considered cycle

ε_u ultimate strain of the combustion chamber wall material

After $N_{qs} = \frac{1}{u_{qs}}$ identical cycles, the ultimate strain ε_u is obtained, which indicates failure. In the simplest case, the ultimate strain ε_u is assumed to be constant over time. A more sophisticated determination of ε_u dependent on temperature and time is described in the following section.

C. Thermal degradation of the material

According to Ref. 10, the ultimate strain ε_u can be defined dependent on the accumulated run time and the temperature of the considered part of the engine:

$$\varepsilon_u = \varepsilon_u(T,\tau) = B_k \cdot \varepsilon_u(T,0) \cdot \left(\frac{\tau_0}{\tau}\right)^{k_e \cdot m_\sigma(T)} \tag{3}$$

with:

B_K parameter, taking into account the 3-dimensionality of the deformation

$\varepsilon_u(T,0)$ temperature dependent initial ultimate strain

τ_0 test time for tensile test

τ accumulated run time of the engine

k_e exponent weighting factor

The thermal degradation exponent m_σ is specified by equation (4):

$$m_\sigma(T) = 0.001 \cdot e^{\beta \cdot T} \tag{4}$$

with: β : temperature weighting factor

D. Total fatigue

The total usage factor u_t is defined as the sum of the cyclic and quasi static usage factors:

$$u_t = u_c + u_{qs} \tag{5}$$

Finally, the total number of cycles until failure N_t is calculated as the reciprocal value of the total usage factor u_t :

$$N_t = \frac{1}{u_t} \tag{6}$$

E. Material parameters

All the material parameters that are needed for the analyses described in the previous sections were completely determined for a Cu alloy, which is used as the inner liner material of a recently tested model combustor at DLR.[6] As the thermal degradation parameters were not determined yet for this Cu alloy, the parameters for a similar Cu alloy as given in Ref. 10 were chosen for the analyses presented in this section.

VI. Optimization of geometric parameters of the chamber wall

A. Problem setting

The objective of the optimization of the geometric parameters is the maximization of the total life time N_t of the combustion chamber wall. However, since optimization procedures in general are designed to minimize functions, the reciprocal value – the total usage factor $u_t = \frac{1}{N_t}$ is selected as the objective function f. Modified geometric parameters are defined as the product of scaling factors and initial parameters:

$$h_c^m = x_1 \cdot h_c^i \tag{7}$$

$$w_c^m = x_2 \cdot w_c^i \tag{8}$$

$$w_f^m = x_3 \cdot w_f^i \tag{9}$$

$$t_w^m = x_4 \cdot t_w^i \tag{10}$$

with:

h_c^m, w_c^m, w_f^m, t_w^m	modified values for the height and width of the cooling channel, the width of the fin and the thickness of the chamber wall, respectively
x_1, x_2, x_3, x_4	scaling factors for the height and width of the cooling channel, the width of the fin and the thickness of the chamber wall, respectively (all scaling factors are set to 1.0 for the initial set)
h_c^i, w_c^i, w_f^i, t_w^i	initial parameters for the height and width of the cooling channel, the width of the fin and the thickness of the wall, respectively

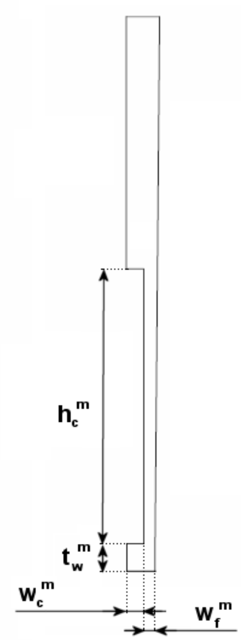

Figure 4. Geometric parameters of the chamber wall.

The geometric parameters h_c^m, w_c^m, w_f^m, t_w^m are also illustrated in Fig. 4. The optimization procedure is aimed to find a design vector x^* so that:

$$f(x^*) = \min_{\underline{x_i} \le x_i \le \overline{x_i},\, x_i = 1,\dots,4} f(x) \tag{11}$$

$$g_i(x) \le \overline{g_i}\,, \qquad i = 1,2 \tag{12}$$

with:

$f(x) = u_t = \frac{1}{N_t}$	objective function
$x^* = (x_1^*, x_2^*, x_3^*, x_4^*)^T$	optimal design variable vector
$x = (x_1, x_2, x_3, x_4)^T$	arbitrary design variable vector in the specified design variables range
$\underline{x_i}$, $\overline{x_i}$, $i = 1,\dots,4$	lower and upper limits for the design variables x_i for $i = 1,\dots,4$, respectively
$g_1(x)$	pressure loss Δp in the cooling channel

$\overline{g_1}$	upper limit for the pressure loss in the cooling channel; chosen equal to the pressure loss of the initial design $\Delta p_i = 20.892$ MPa)
$g_2(x)$	wall temperature at point D
$\overline{g_2}$	upper limit for the wall temperature at point D; chosen as $T = 1100\ K$

The constraints g_1 and g_2 ensure that the pressure loss of the optimal design is not higher than the pressure loss in the initial configuration and that the temperature at point D does not exceed the melting temperature of the combustion chamber wall material.

B. Preliminary analysis of the influence of the design parameters

For certain optimization problems, one or more of the design variables can be determined a priori. Therefore, the influence of the design variables on the objective function and the constraints of the problem are discussed in Table 2.

Table 2. Influence of the design parameters on the objective function and the constraints.

design parameter change	**influence on**			
	thermal loading of the chamber wall	**mechanical loading** of the chamber wall	**life time** of the chamber wall	**pressure loss** in the cooling channel
decreasing **thickness of the chamber wall**	improved cooling caused by increased heat flux: → **loading decreases**	decreasing resistance to pressure difference cooling channel-combustion chamber: → **loading increases**	no general statement possible	minimal influence
decreasing **width of the cooling channel**	improved cooling caused by decreasing cross section of cooling channel: → **loading decreases**	increasing resistance to pressure difference cooling channel – combustion chamber: → **loading decreases**	lower thermal and structural loading: → **life time increases**	reduction of cross section of cooling channel: → **pressure loss increases**
decreasing **height of the cooling channel**	improved cooling caused by decreasing cross section of cooling channel: → **loading decreases**	minimal influence	decreased thermal loading: → **life time increases**	reduction of cross section of cooling channel: → **pressure loss increases**
decreasing **width of the fin**	decrease of heat transfer cross section of the fin and decrease of coolant velocity: → **loading increases**	softer connection between inner chamber wall and steel coating: → **loading decreases**	no general statement possible	increase of number of cooling channels: → **pressure loss decreases**

The considerations shown in Table 2 imply that none of the design parameters can be determined a priori. Indeed either the influence of the design parameter has an opposite effect on mechanical and thermal loading or the influence on the constraints penalizes possible improvements in the thermal and mechanical loading. Therefore, no reduction of the complexity of this optimization problem is possible and therefore, all the design variables have to be included in the optimization process. Two different optimization methods are described and compared in the following subsections.

C. Conjugate Gradient optimization method

The applied optimization procedure consists of two steps: Transformation of the constrained minimisation problem into an unconstrained minimisation problem by means of penalty terms and solution of the unconstrained minimisation problem by a standard Conjugate Gradient method.[11]

1. Transformation of the constrained minimisation problem into an unconstrained minimisation problem

Penalty functions X_i and G_i are used in order to transform the constrained minimisation problem (11), (12) into an unconstrained minimisation problem with the dimensionless objective function $F(x)$:

$$F(x,p) = \frac{f\ (x)}{f_0} + \sum_{i=1}^{4} X(x_i) + p \sum_{j=1}^{2} G(g_j(x)) \tag{13}$$

with:

f_0	reference objective function value
p	adaptively chosen penalty parameter
$X(x_i)$	exterior penalty functions for design variables
$G(g_j(x))$	extended interior penalty functions for state variables

2. Solution of the unconstrained minimisation problem

Each iteration step of a gradient based optimization procedure can be split into 3 parts: Approximation of the gradient; choice of a gradient based search direction and update of the design variables. For the optimization of the model combustion chamber, the Conjugate Gradient method according to Polak and Ribiére[11] was used.

- Approximation of the gradient of the objective function F

As the gradient can not be determined analytically, a forward difference quotient is used to approximate the gradient of the dimensionless objective function F of the unconstrained minimisation problem:

$$\nabla F = \left(\frac{\partial F(x)}{\partial x_1}, \ldots, \frac{\partial F(x)}{\partial x_4} \right)^T \tag{14}$$

$$\frac{\partial F(x)}{\partial x_i} \approx \frac{F(x + \Delta x_i e_i) - F(x)}{\Delta x_i} \tag{15}$$

with:

e_i	vector with 1 in its *i*-th component and 0 for all other components
Δx_i	small increment for *i*-th design variable

- Determination of a search direction

At the first iteration step, the negative gradient is used as a search direction d_0 :

$$d^0 = -\nabla F(x^0) \tag{16}$$

with: x^0 : initial design variable vector.

As the design variables are corrective factors to the initial design, the initial design variable vector is the unit vector: $x^0 = (1,1,1,1)^T$. At subsequent iterations, the negative gradient is modified by adding the previous search direction d_{j-1} , scaled by a factor r_j :

$$d^j = -\nabla F(x^j) + r^j d^{j-1} \tag{17}$$

$$r^j = \frac{(\nabla F(x^j) - \nabla(F(x^{j-1})) \cdot \nabla F(x^j)}{\nabla F(x^{j-1}) \cdot \nabla F(x^{j-1})} \tag{18}$$

Occasionally, the Conjugate Gradient algorithm is restarted by choosing the steepest descent search direction instead of the conjugated direction.

- Update of the design variable vector

  Finally, the new design variable vector x^{j+1} is obtained by the following equation:

$$x^{j+1} = x^j + s^j d^j \, , \qquad j=0,1,2,\ldots \tag{19}$$

The line search parameter s^j corresponds to the minimum value of F in the search direction d^j .

D. Gradient free optimization method

Each calculation of the life time for a given design variable vector x requires full thermo mechanical and nonlinear structural analyses of the combustion chamber as described in the previous sections. Therefore, an optimization procedure has to be used, which requires as little calculations of the objective function $f(x)$ and the constraint functions $g_i(x)$ as possible. The following two-step optimization method fulfils this requirement better than the Conjugate Gradient method, because (after performing the calculation of $f(x)$ and *for* a few number of randomly generated design sets at the very beginning of the procedure) only one calculation of $f(x)$ and $g_i(x)$ per optimization step is necessary. This optimization method can be split into two parts: approximation of $f(x)$ and $g_i(x)$ by quadratic functions and minimization of the quadratic objective function $f_q(x)$ and quadratic constraint functions $g_{i,q}(x)$ by a sequential unconstrained minimisation technique.

1. Approximation of the objective function and the constraints by quadratic functions

The objective function is approximated by functions of the following form:

$$f(x) \approx f_q(a_i^*, b_{ij}^*, x) = a_0 + \sum_{i=1}^{4} a_i^* x_i + \sum_{i=1}^{4}\sum_{j=1}^{4} b_{ij}^* x_i x_j \tag{20}$$

The constraint functions $g_i(x)$ are approximated by similar quadratic functions $g_{i,q}(x)$, *i =1,2*. The coefficients a_i^* and b_{ij}^* are determined by a least squares fit:

$$\sum_{k=1}^{n_d} w^k \left(f(x^k) - f_q\,(a_i^*, b_{ij}^*, x^k)\right)^2 = \min_{a_i, b_{ij}} \sum_{k=1}^{n_d} w^k \left(f(x^k) - f_q\,(a_i, b_{ij}, x^k)\right)^2 \tag{21}$$

with:

n_d number of analysed design sets

x^k k-th design set

w^k weight factor for k-th design set

2. Sequential unconstrained minimization technique

By use of extended interior penalty functions $X(x_i)$ and $G(g_{j,q}(x))$, the constrained minimisation problem is transformed into a series of unconstrained minimisation problems with the objective function $F_q(x, p_k)$:

$$F_q(x,p_k) = \frac{f_q(x)}{f_0} + p_k\left(\sum_{i=1}^{4} X(x_i) + \sum_{j=1}^{2} G(g_{j,q}(x))\right) \tag{22}$$

with: p_k, $k=1,2,\ldots$ series of increasing penalty parameters

E. Optimization results for the 2d plane strain model

Although the total usage factor u_t was used as an objective function, the evolution of the inverse objective function $N_t = 1/u_t$ (estimated total life time until failure) for the optimization with the 2d plane strain model is shown in Fig. 5.

The graph shows the results of all life time analyses, including the step size search analyses of the Conjugate Gradient method and some random design set analyses at the beginning of the gradient free optimization procedure. Therefore, the objective function does not show a monotonic behaviour. Also, not all of the analysed design sets fulfil the given constraints. Therefore, the design sets with the minimum objective function value out of all sets, fulfilling the constraints are marked in the given figure. Both methods lead to an increase of the estimated number of cycles until failure N_t by a factor of more than 2.

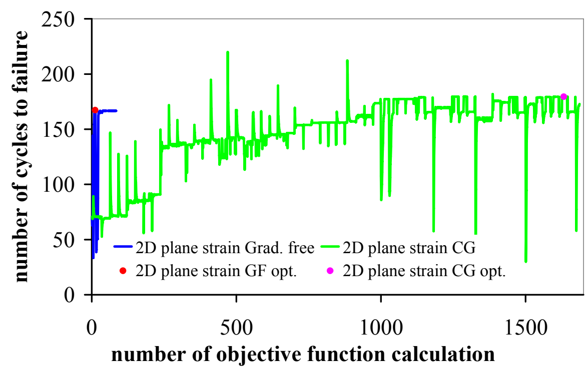

Figure 5. Evolution of the estimated number of cycles until failure N_t for two different optimization procedures using the 2 d plane strain model.

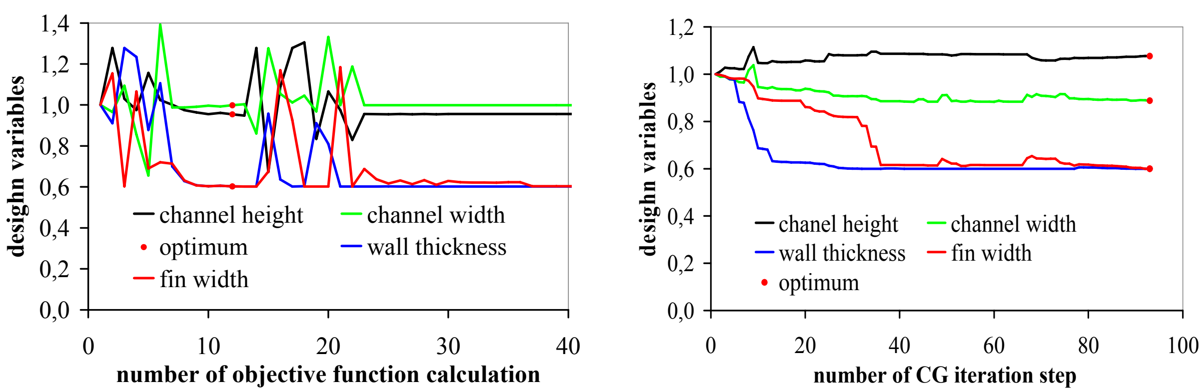

Figure 6. Evolution of the design parameters for the gradient free method (left) and the Conjugate Gradient method (right) using the 2d plane strain model.

In case the gradient free method is used, the optimal result (167 cycles to failure) is obtained after 12 design sets. For the Conjugate Gradient optimisation run, 1632 design sets were analysed until the optimal solution (179 cycles to failure) was obtained. From these numbers it can be concluded, that for this optimization problem, the efficiency of the gradient free optimisation procedure in comparison with the Conjugate Gradient method is more than 100 times higher as the efficiency of the Conjugate Gradient method.

The evolution of the design parameters during the optimization with the 2d plane strain model is shown in Fig. 6. A more convenient visualisation of the obtained designs of the combustion chamber wall, including also the temperature distribution in the chamber wall during the hot run phase, is given in Fig. 9.

F. Optimization results for the 2d generalized plane strain model

The evolution of the inverse objective function $N_t = \frac{1}{u_t}$ during the optimization with the 2d generalized plane strain model is shown in Fig. 7.

As in the previous subsection, the design sets with the minimum objective function value out of all sets, fulfilling the constraints are marked in the given figure. The gradient free method leads to an increase of the estimated number of cycles until failure N_t by a factor of more than 1.6, whereas the Conjugate Gradient method leads to an increase of this number by a factor of more than 2. In case the gradient free method is used, the optimal result (159 cycles to failure) is obtained after 48 design sets. For the Conjugate Gradient optimisation run, 923 design sets were analysed until the optimal solution (207 cycles to failure) was obtained. The efficiency of the gradient free optimisation procedure in comparison with the Conjugate Gradient method is more than 20 times higher as the efficiency of the Conjugate Gradient method. However, the optimization result of the Conjugate Gradient method is much better than the optimization result, obtained by the gradient free method.

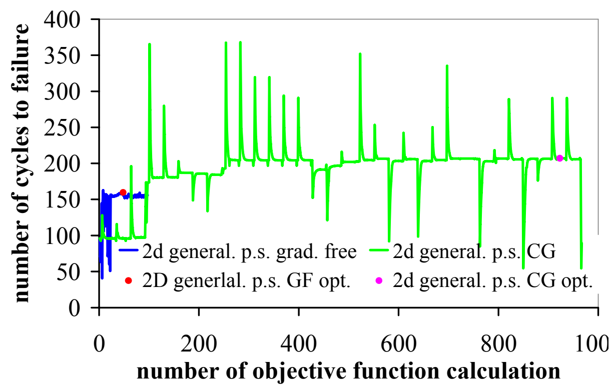

Figure 7. Evolution of the estimated number of cycles until failure N_t for two different optimization procedures for the 2d generalized plane strain model.

The evolution of the design parameters during the optimization with the 2d generalized plane strain model is shown in Fig. 8.

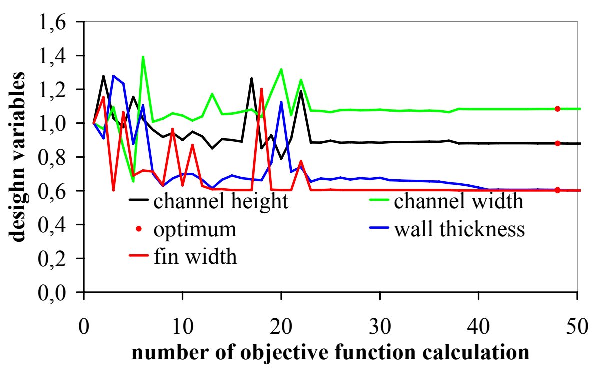

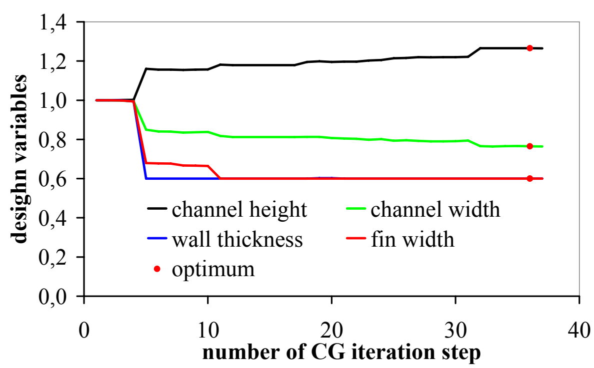

Figure 8. Evolution of the design parameters for the gradient free method (left) and the Conjugate Gradient method (right) for the generalized plane strain model.

G. Discussion of the optimization results

The different optimized design parameters for the gradient free as well as for the Conjugate Gradient optimization methods and the two different considered 2d models (plane strain and generalized plane strain) are shown in Figs. 6, 8 and 9. Obviously, the wall thickness and the fin width are reduced to the lower design variable limits (factor of 0.6 to the initial design) for both Finite Element models and both optimization methods.

The advantage of the reduction of the wall thickness is obvious, as it leads to a lowering of the wall temperatures and therefore, to a decrease of the cyclic thermal strain, which is the main driver for the low cycle fatigue of the chamber wall. Obviously, this decrease of the cyclic straining compensates for the increased mechanical loading of the chamber wall.

The activation of the design variable constraints for the wall thickness and the fin width leads to the conclusion that the unconstrained result of an optimization of these design variables would lead to even lower values of these variables. However, for the following reasons these design variables can not be allowed to get arbitrarily small:

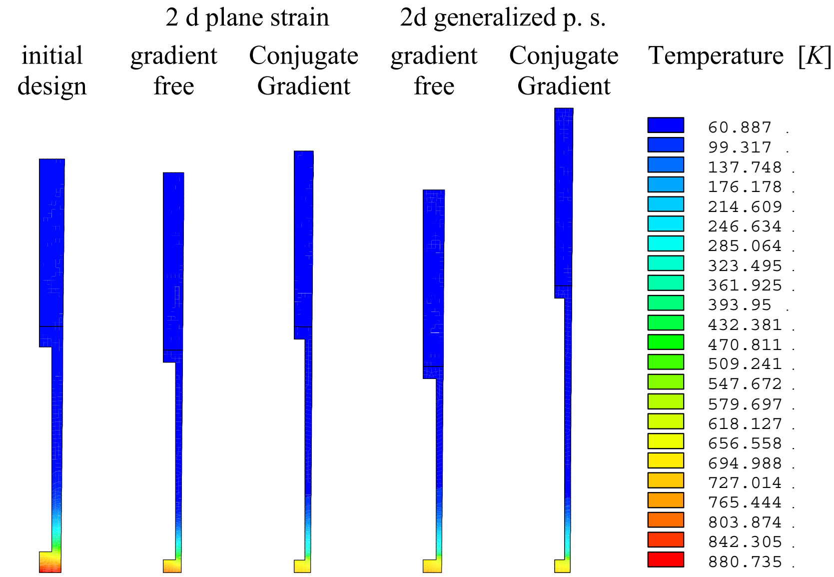

Figure 9. Dimensions and thermal fields during the hot run for the initial and the optimized design sets.

- The minimum thickness of the combustion chamber wall is limited by 2 factors, which were not taken into account for the current structural analysis: the maximum size of defects in the wall material and tooling tolerances during the production process. Both of these factors could lead to a defect of the combustion chamber wall immediately after production already, if the wall thickness is small enough.
- The minimum thickness of the fin is certainly limited on the size of force, applied by the milling tool during the production process of the cooling channel. In case of a very small thickness of the fin, this force could lead to a deformation of the fin during the production process. On top of that, the compressive radial forces, caused by the temperature differences between the inner Cu liner (that tends to expand during the hot run) and the outer Ni jacket (that tends to contract due to the low bulk temperature of the coolant during the hot run) could lead to a buckling of the fin in case the fin width is too small. As a symmetry boundary condition is applied at the middle plane of the fin, this possible buckling can not be obtained as a result of the Finite Element analysis.

For the other two optimization parameters different results are obtained for the different optimization methods: the optimization with the Conjugate Gradient method resulted in combination with both of the 2d models in a reduction of the width and an increase of the height of the cooling channel, whereas the opposite can be observed for the optimization with the gradient free method. As the Conjugate Gradient method with both of the 2d models resulted in a stronger increase of the number of cycles to failure, the Conjugate Gradient optimization results have to be preferred. The life time advantage of a reduction of the width of the cooling channel was discussed already in Table 2. In case of a fixation of all the other design parameters, this would lead to an increase of the pressure loss in the cooling channel, which was ruled out for the optimization process by the constraint $g_1(x)$ in equation (12). However, in case the reduction of the cooling channel width is compensated by an increase of the cooling channel height, the pressure loss can be kept constant while the number of cycles until failure is increased.

This optimization result justifies the currently observed trend to high aspect ratio cooling channels, which is mainly limited by the production technology of the cooling channels. As for high aspect ratio cooling channels the thermal stratification effect becomes more and more important, the optimization results will have to be confirmed by an improved analysis of the thermal field in the cooling channel and the combustion chamber wall. As the coupling of a fully 3d CFD analysis of the coolant flow in the cooling channel with the Conjugate Gradient method is still too time consuming f an improved 1d thermo-mechanical fluid flow analysis - coupled with a thermal analysis of the combustion chamber wall will have to be used for this purpose.

VII. Summary

Finite Element coupled optimization algorithms for the enlargement of the life time of a combustion chamber wall were suggested. Firstly, all the necessary sub steps - such as thermal analysis, non-linear structural analysis, life time estimation and optimization methods were discussed. Furthermore, a preliminary consideration of the influence of the different design parameters of the objective function and the constraints was performed. Finally, the influence of the choice of the 2d model (plane strain or generalized plane strain) was discussed. As far as the choice of the optimization algorithm (gradient free or Conjugate Gradient optimization method) is concerned, the gradient free method can be recommended to find optimized combustion chamber wall parameters in a comparatively short time, whereas the life time improvement potential of the optimization is higher in case the much slower Conjugate Gradient method is applied.

VIII. Outlook

Future developments at DLR will aim at the improvement of the accuracy of the thermal and structural analyses and life time estimation methods. A series of improvements is possible for the thermo mechanical analysis and life time estimation of the combustion chamber wall:

- Taking into account thermal stratification effects of the coolant flow in the cooling channel,
- application of an improved material model including a combination of a multilinear isotropic hardening and nonlinear kinematic hardening[12,13] instead of the currently used material model, assuming only a multilinear elasto-plastic material behavior with isotropic hardening,
- structural analysis of a series of cycles,
- taking into account additional effects such as the hydrogen embrittlement and the blanching of the material.

References

[1]Kuhl, D., Riccius, J.R. and Haidn, O.J., "Thermomechanical analysis and optimization of cryogenic liquid rocket engines," *AIAA Journal of Propulsion and Power*, Vol. 18, No. 4, 2002, pp. 835-846.

[2]Riccius, J.R., Hilsenbeck, M.R. and Haidn, O.J., "Optimization of geometric parameters of cryogenic liquid rocket combustion chambers," *37th AIAA/ASME/SAE/ASEE JPC*, *AIAA-01-3408*, 2001

[3]Riccius, J.R., Jouinot, P. and Gantschenko, V.: "Elasto-plastic and fatigue tests of a typical combustion chamber material with different sample geometries. *4th International Conference on Launcher Technology "Space Launcher Liquid Propulsion",* Liege Belgium, (2002)

[4]Riccius, J.R. and Haidn, O.J., "Determination of linear and nonlinear parameters of combustion chamber wall materials," *39th AIAA/ASME/SAE/ASEE Joint Propulsion Conference, AIAA-03-4901*, 2003

[5]Bartz, D.R., "A simple equation for rapid estimation of rocket nozzle convective heat transfer coefficients," *Jet Propulsion*, 27:49–51, 1957.

[6]Woschnak, A., Suslov, D. and Oschwald, M., "Experimental and numerical investigations of thermal stratification effects," AIAA 2003-4615, *39th AIAA/ASME/SAE/ASEE JPC*, 2003 Huntsville, AL

[7]Riccius, J.R., Haidn, O.J. and Zametaev, E.B., "Influence of time dependent effects on the estimated life time of liquid rocket combustion chamber walls," AIAA 2004-3670, *40th AIAA/ASME/SAE/ASEE Joint Propulsion Conference*, July 2004 Fort Lauderdale, Florida

[8]Oschwald, M., Suslov, D. and Woschnak, A., „Einfluss der Temperaturabhängigkeit der Materialeigenschaften auf den Wärmehaushalt in regenerativ gekühlten Brennkammern," DGLR-2004-111, *Deutscher Luft- und Raumfahrtkongress*, Dresden, September 2004

[9]Jouinot, P., Gantschenko, V., Inglebert, G. and Riccius, J., "Material damage induced by environment and temperature and identification process," *Forth European Congress on Computational Methods in Applied Sciences and Engineering*, ECCOMAS 2004, P. Neittaanmäki, T. Rossi, S. Korotov, E. Oñate, J. Périaux, and D. Knörzer (eds.), Jyväskylä, July 2004

[10]Rudis, M.A. and Riccius, J.R., "Liquid rocket engine component failure probability and residual life prediction at thermal and mechanical cyclic loading," *Forth European Congress on Computational Methods in Applied Sciences and Engineering*, ECCOMAS 2004, P. Neittaanmäki, T. Rossi, S. Korotov, E. Oñate, J. Périaux, and D. Knörzer (eds.), Jyväskylä, July 2004

[11]Polak, E. and Ribiére, G. "Note sur la convergence de méthodes de directions conjuguées," Revue Française d´Informatique et de Recherche Opérationnelle 16, 35-43, 1969

[12]Chaboche, J.L., "Equations for Cyclic Plasticity and Cyclic Viscoplasticity", *International Journal of Plasticity*, Vol. 7, pp. 247-302 (1989).

[13]Chaboche, J.L., "On Some Modifications of Kinematic Hardening to Improve the Description of Ratcheting Effects", *International Journal of Plasticity*, Vol. 7, pp. 661-678 (1991).